IEEE Access
Multidisciplinary | Rapid Review | Open Access Journal

SPECIAL SECTION ON URBAN COMPUTING AND INTELLIGENCE

Received October 9, 2019, accepted November 16, 2019, date of publication December 13, 2019,
date of current version December 26, 2019.

Digital Object Identifier 10.1109/ACCESS.2019.2959557

Flooding Level Classification by Gait Analysis of Smartphone Sensor Data

UJJAWAL K. PANCHAL, (Member, IEEE), HARDIK AJMANI, AND SAAD Y. SAIT, (Member, IEEE)
Department of Computer Science and Engineering, SRM Institute of Science and Technology, Kattankulathur 603203, India
Corresponding author : Saad Y. Sait (saady@srmist.edu.in)

ABSTRACT Urban flooding is a common problem across the world. In India, it leads to casualties every year, and financial loss to the tune of tens of billions of rupees. The damage done due to flooding can be mitigated if the locations deserving attention are known. This will enable an effective emergency response, and provide enough information for the construction of appropriate storm water drains to mitigate the effect of floods. In this work, a new technique to detect flooding level is introduced, which requires no additional equipment, and consequent installation and maintenance costs. The gait characteristics in different flooding levels have been captured by smartphone sensors, which are then used to classify flooding levels. In order to accomplish this, smartphone sensor readings have been taken by 12 volunteers in pools of different depths, and have been used to train machine learning models in a supervised manner. Support vector machines, random forests and naïve bayes models have been attempted, of which, support vector machines perform best with a classification accuracy of 99.45%. Further analysis of the most relevant features for classification agrees with our intuition of gait characteristics in different depths.

INDEX TERMS Activity recognition, smartphone sensors, gait analysis, machine learning, flooding level detection.

I. INTRODUCTION

Flooding during heavy rains can be disastrous in urban areas with poor planning. It leads to loss of life and property, infrastructural, and economic damage. During a flooding disaster, it is useful to determine the level of flooding in order to rush emergency response to the required location using an appropriate route. Further, knowledge of the flooding level leads to better urban planning and remedial measures to mitigate the effect of floods. This paper introduces a new technique to detect the level of flooding using smartphone sensors.

Traditionally, flooding detection has been done using a satellite-based remote sensing technique called Synthetic Aperture Radar (SAR) (e.g. [1] and [2]). However, performance using this technique deteriorates significantly in the case of an urban settlement. This is because much of the ground area is blocked by establishments such as buildings, walls, or big vehicles.

Frequently, several commuters are left with no option but to wade through water. Gait characteristics of commuters in different flooding depths, can be captured by smartphone sensors, which can then be used to classify the flooding level at a particular location. This obviates, to some extent, the need for additional equipment, installation and maintenance costs; further, the ubiquitous nature of the smartphone aids in the construction of a 'flood map' with level of flooding shown at different locations, which would be handy for emergency response and construction of storm water drains. It is envisaged that smartphone users would just open an app while walking in a flooded region, which would record sensor readings, classify the level of flooding, and send the level of flooding and location to a central server.

Use of smartphone sensors for gait analysis and human activity recognition (e.g. sitting, standing, lying down, walking, jogging etc.) is an active area of research with a variety of applications in the fields of medicine, fitness, sports, and biometric verification. From among all smartphone sensors, it has been noted in [3] that accelerometer and gyroscope signals provide the most information about human movement. In this work, smartphone sensor data (based on accelerometer, gyropscope and magnetometer sensors) has been collected by a group of 12 volunteers using AndroSensor, for individuals walking in water at different depths. Time-domain (e.g. mean, variance) and frequency domain features (e.g. sum of FFT coefficients) have been extracted from windows of data. Random Forests, support vector machines and naïve

The associate editor coordinating the review of this manuscript and approving it for publication was Lu Liu.

bayes models have been attempted of which support vector machines offer the best performance with up to 99.45% classification accuracy. An analysis of the most relevant features for classification has been performed, which justifies the intuition of the differences between gaits at different flooding levels.

The remaining sections of the paper are organized as follows; Sec. II provides a background for the motivation behind this work; Sec. III discusses related work with respect to activity recognition using smartphone sensors; Sec. IV discusses the forces involved during human movement in water; Sec. V describes how data was collected. Sec. VI describes the features extracted for building machine learning models; Sec. VII explains the machine learning models and performance metrics used; Sec. VIII evaluates the performance of the algorithms and finally Sec. IX concludes the paper.

II. BACKGROUND

Urban flooding is a severe problem in India. The financial loss ensuing out of damage to infrastructure runs into tens of billions of rupees [5]; daily life is also affected due to confinement of people at homes, which in turn affects the economy.

The causes of flooding are many. Firstly, improper city planning - in many cases water bodies have been converted to settlement areas, which naturally get flooded with excessive rainfall; water flow gets blocked due to encroachments in urban areas; surface sealing in urban areas due to impervious surfaces in the form of pavement and buildings increases runoff. Secondly, drainage system is ill-equipped to handle excessive rainfall, drains get blocked by solid waste, and obstructions from city constructions like bridges and flyovers. Thirdly, climate has changed with the result that more rainfall in a shorter span of time has become a more frequent occurrence [4].

The state of the art for flood detection is a remote sensing technique called Synthetic Aperture Radar (SAR). It is essentially a technique in which high resolution images are obtained from a side looking moving satellite using radar [1], [2]; images can be taken during day and night, and even in the case of bad weather, and near-real time detection can be achieved using TerraSAR-X, a satellite with an orbit of 1.6 hrs. However, much of the urban area blocked by buildings cannot be classified correctly; algorithms are able to correctly classify 76% of the flooded pixels visible to the radar [1], which means there is scope for improvement. Detection of flooding level by identifying gait characteristics in that flooding level (using smartphone sensors) has the potential for good classification performance (as will be demonstrated later in the paper); due to the ubiquitous nature of the smartphone, flooding information at all locations may be obtained; further, all this can be accomplished at minimal cost to the government.

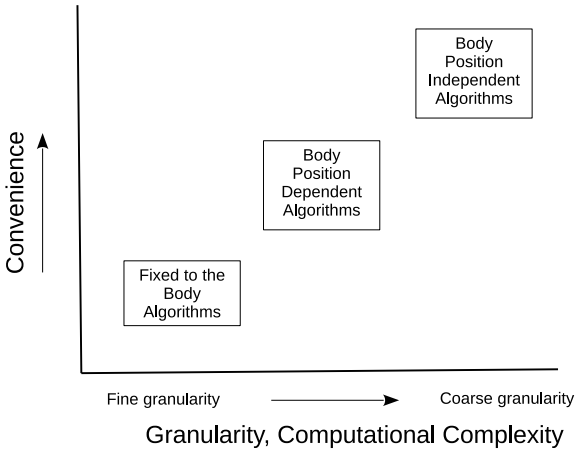

FIGURE 1. Comparison of FBAs, BPDAs and BPIAs.

III. RELATED WORK

Classification of flooding level based on gait characteristics is similar to human movement monitoring. In this section, a survey of human movement monitoring has been performed. However, we restrict the discussion to smartphone sensors rather than wearable sensors, which have been used in the likes of [6]–[9].

Reference [10] surveys the evolution of smartphone sensors for monitoring human movement. They divide the research work into 3 broad categories. *Fixed to the body algorithms* (FBA) require the smartphone to be in a fixed position and orientation; basically, they require the smartphone to be strapped to the body. *Body position dependent algorithms* (BPDAs) require the smartphone to be placed in a fixed position, but do not require the orientation to be fixed, for e.g. placing the smartphone in the pockets on the hip or the chest. *Body position independent algorithms* (BPIAs) do not require the smartphones to be placed either in a fixed position or orientation. Fig. 1 depicts how these classes of algorithms fare with regard to convenience of use and granularity of classification. While FBAs are somewhat inconvenient to use, as the smartphone should be strapped to the body at a fixed position and orientation, in the case of BPDAs, orientation may change, while in the case of BPIAs, both orientation and position may change. The convenience of BPIAs comes at the cost of granularity of the classification task, e.g. distinguishing between walking and walking up the stairs performs poorly [11]; BPIAs are also computationally intensive when compared to FBAs and BPDAs. On the other hand FBAs can categorize tasks of finer granularity compared to BPDAs and BPIAs e.g. identifying a variety of movements [12] which aid in estimating energy expenditure, identifying movements specific to certain sports (soccer, hockey) [13], and evaluating exercises performed in a gymnasium [14]. In this work, the FBA approach has been used; the benefits of fine granularity of FBAs has been preferred over the coarse granularity of BPIAs, as it is desired to differentiate

between gait characteristics in different depths; even-though BPIAs offer convenience of use, this factor is relatively less important because a reading taken over a period of 5s is sufficient for classification.

A subarea of human movement monitoring that is relevant to this research work is *gait analysis*, which involves "a measurement, description and assessment of quantities that characterize human locomotion" [15]. In this area, smartphones have been used to predict the health status of individuals suffering from chronic obstructive pulmonary disease (COPD) [16], by measuring the speed of movement of an individual, as this is an indication of his/her health. Others have used smartphones to detect abnormal gait patterns which may be used as an alert to indicate susceptibility to falls [17] or a developing Parkinson's disease [18]. Gait-based user verification and authentication is another area where smartphones have been used; they are useful to detect theft of smartphones, faking of gait (e.g. to lower health insurance costs) and user spoofing attacks to claim healthcare benefits or to find fault with the successful operation of mobile healthcare systems [19], [20], [22]–[25]. Reference [21] analyzes the gait to determine the level of intoxication of an individual e.g. 0-2 drinks, 3-6 drinks or more than 6 drinks, with an accuracy of 70%.

Another subarea of human movement monitoring, closely related to gait analysis, is human activity recognition (HAR); activities like sitting, standing, walking, running, ascending and descending stairs may be recognized and enable the computation of energy expenditure, which can then be used to evaluate individuals with obesity and diabetes. As flooding-level detection also involves distinguishing between different types of walking (based on flooding level), the authors review the techniques used in HAR. Approaches to HAR typically use a window of data [26]–[32] spanning a few seconds to classify the activity by computing statistical features over the window like mean, median, variance, etc. These are also referred to, as *time domain* features. References [27], [29]–[31] include autoregression coefficents while [26] includes autocorrelation function as a feature to model the correlation between data points in close proximity to one another. *Frequency domain* features like spectral energy, fast fourier transform coefficients have also been used [26], [28]. Classifiers used are naïve bayes [26], [29], decision trees [26], [33], k-nearest neighbours (kNN) [28], [29], deep belief networks [30] and support vector machines [26], [33]. As the sensor readings represent a time series, [34] uses a convolutional neural network (CNN) in order to make use of correlation between data points in close proximity; moreover they make use of a multi-layer CNN to extract complex features. Similarly, [35] uses hidden markov models (HMMs) to model the sequence of data points; their approach is hierarchical, the first level of which reads raw data and identifies an action (e.g. walking, standing, etc.) and the second level takes a sequence of actions as input and identifies an activity (e.g. shopping, travelling by bus).

Various sensors have been used in the area of activity recognition using smartphone sensors - accelerometer, gyroscope, magnetometer, barometric pressure sensor, audio-visual components (camera, microphone) and location-based sensors (e.g. WiFi, Bluetooth, GPS). Among these, accelerometer, gyroscope, magnetometer and barometric pressure sensor consume less power when compared to the others. Further, it has been noted that accelerometer and gyroscope signals provide the most information about human movement [3]. In this work, accelerometer and gyroscope sensors have been used; both time-domain and frequency domain features have been extracted; even-though frequency domain features are more computationally expensive than time domain features [36], unlike human activity recognition, flooding level detection is a one time activity over a span of 5s that is triggered by the user when required. Support vector machines, random forests and naïve bayes models have been used to classify examples.

IV. HUMAN MOVEMENT IN WATER

A summary of the forces acting in water will be provided in this section. The forces acting on individuals in water (shown in Fig. 2a, Fig. 2b and Fig. 2c) are:

1) *Force due to Gravity*: Force exerted on the individual due to Earth's gravitational pull.
2) *Buoyant Force*: Upward force exerted by the fluid (water) on the object immersed in it in a direction opposing force due to gravity. It increases with depth.
3) *Drag Force*: Force exerted by the liquid in a direction opposite to relative motion of the body with respect to the liquid. It increases with cross-sectional area of immersed object. In the case of human movement in water, larger depths cause larger drag, as the surface area immersed inside water increases.

The forces acting on the smartphone are (see Fig. 2d):

1) *Force due to Gravity*: Force exerted on the smartphone due to Earth's gravitational pull.
2) *User Exertion*: Force exerted by the user on the smartphone. The direction of user exertion varies, as indicated in the figure.

The above forces affect the smartphone sensor readings. It may be noted that drag force and buoyancy do not directly act on the smartphone, as the smartphone is kept out of water. However, they influence the user exertion on the smartphone.

V. DATA COLLECTION

The authors are not aware of any data set available for flooding-level detection, and have therefore, collected smartphone sensor data for this purpose; data was recorded using smartphones by volunteers, who obtained the readings from several swimming-pools with different depths of water, and on land as well. Samsung Galaxy S8+ and Lenovo Zuk Z2 plus were used to record the data, both of which are based on Android operating system. AndroSensor, a freely available app for Android, was used to take the readings

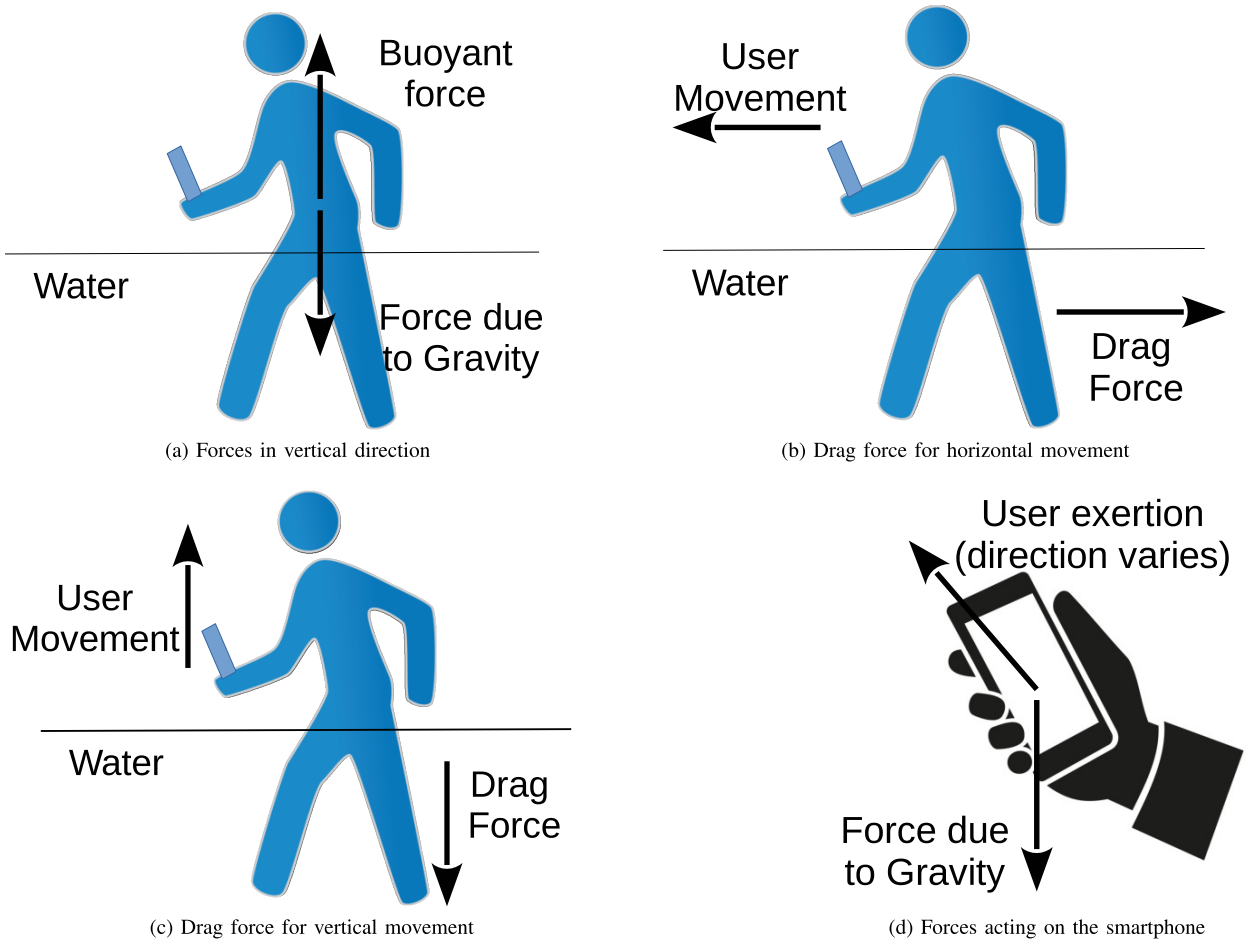

(a) Forces in vertical direction

(b) Drag force for horizontal movement

(c) Drag force for vertical movement

(d) Forces acting on the smartphone

FIGURE 2. Forces acting on a human moving in water.

with updating interval (measure of how frequently readings are taken) set to 'very fast' and recording rate (measure of how frequently readings are updated to data file) set to 10Hz. A group of 12 volunteers (with body mass indices in the range 17-30.6, standard deviation of 4.13) took the readings in swimming pools of different depths. Readings were taken by keeping the mobile phones in the position shown in Fig 3, with the display facing the volunteer; the smartphone could be held in either hand. The following smartphone sensors were activated before recording data:

1) *Gravity Sensor:* It provides the projection of acceleration due to gravity on the three axes of the mobile phone. These values will be represented as g_x, g_y and g_z. Force due to gravity is constant in the direction of the earth. Smartphone users were instructed to hold it vertical, which means that ideally only g_y is non-zero. In reality, there is always some deviation from the ideal position, which results in non-zero values for g_x and g_z as well, and smaller values than 9.8 for g_y. This frequently happens due to disturbances in water, which cause the users to tilt their phones.
2) *Linear Acceleration Sensor:* It provides accelerations along axes of mobile phone that are not caused by gravity; these are a result of user exertion. These values will be represented as a_x, a_y and a_z.
3) *Gyroscope Sensor:* It provides the angular velocity with respect the axes of the mobile phone. These will be denoted as ω_x, ω_y and ω_z.

It may be noted that gravity and linear acceleration sensors may be implemented as software sensors, whose values are derived from the accelerometer, gyroscope and magnetometer.

The readings mentioned above were taken while walking in pools with depths 4.5ft, 2.5ft, 0.19ft as well as on dry land. While the 4.5ft and 2.5ft were taken in swimming pools, the 0.19ft reading was taken by flooding a washroom with water. Volunteers were requested to obtain readings for walking straight a few metres, at the end of which, they were to stop the recording; turnings were not recorded. The number of readings taken, for different depths, has been shown in Table 1. The method of extracting the examples from raw readings will be explained in the next section.

VI. FEATURE EXTRACTION

As mentioned before, sensor data was collected at a recording rate of 10Hz. The standard approach in the case of HAR

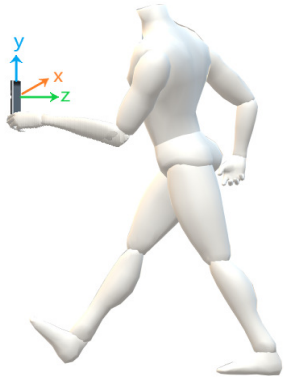

FIGURE 3. Posture of a volunteer walking with smart phone in hand.

TABLE 1. Details of readings and examples for each depth.

Depth	No. of Readings	No. of examples
0 feet	3503	140
0.19 feet	5372	214
2.5 feet	3520	140
4.5 feet	10223	408

using smartphones has been to extract time and frequency domain features from a window of data; further 50% overlap is permitted between consecutive windows [10]. In this work, a window size of 5s has been used; this means 50 consecutive readings when data is recorded at 10Hz, with an overlap of 25 readings between consecutive examples. This window size was chosen in order to enable capture of frequency components present in the gait, as a single step would typically take between 0.5-1s. The number of examples obtained by using the above procedure has been shown in Table 1.

Time domain features extracted from each window are mean, median and variance. Frequency domain features extracted have been explained below:

1) *Sum of FFT Coefficients:* Fourier Transform converts a set of values from their original (space or time) domain to the frequency domain. Discrete Fourier Transform (DFT) decomposes a signal in terms of its frequency components. Fast Fourier Transform (FFT) is an efficient way of computing DFT. The first five coefficients found using the FFT representing lower frequencies are summed. A higher value of the sum of FFT coefficients indicates a better frequency response at these lower frequencies.
2) *Spectral Energy:* It is the sum of squared FFT coefficents normalized by length of the window. The spectral energy is proportional to the energy of the signal E specified in Eq. 1, where $x(n)$ is the signal value of n^{th} sample, and N is the number of samples in the window. This means that large signal magnitudes increase the spectral energy of a signal.

$$E = \sum_{n=0}^{N} |x(n)|^2 \tag{1}$$

Three sensor readings have been considered (as mentioned before) - linear acceleration, gravity and angular velocity. For each, there are components along 3 directions of the mobile phone, and for each of these 5 features have been extracted (time and frequency domain features) over a window of data; this means 45 features for each window of data, therefore each training example contains 45 features.

VII. EXPERIMENTAL SETUP

Preprocessing performed, machine learning models and performance metrics used are described in this section.

A. PREPROCESSING

All features f_i were first normalized by subtracting the means μ_i and dividing by respective standard deviations σ_i as shown in Eq. 2. This was done in order to prevent the results from being biased towards features with large magnitudes.

$$f_i' = \frac{f_i - \mu_i}{\sigma_i} \tag{2}$$

B. MACHINE LEARNING MODELS

In this work, random forests, naïve bayes and support vector machine classifiers were used to classify the examples; the main consideration in the choice of these classifiers (over neural networks, CNNs, HMMs or kNN) was the simplicity of the models which have fewer training parameters and are therefore more suitable for a small data set. Another advantage of these models over neural networks is the lower computational and energy requirements, which render them more suitable for implementation in the smartphone. These models have been implemented using python sklearn library (explained below).

1) RANDOM FORESTS

Random forests (RF) is an ensemble of decision trees. The training data for each tree is obtained by choosing each example randomly with replacement; further, the next feature to be chosen for the split is restricted to a subset of the features. In this fashion, a number of trees are generated; the majority vote of all trees is the predicted category of the random forest. In this manner, random forests try to improve the classification accuracy as well as prevent overfitting.

The parameters used for random forests have been listed in Table 2. Entropy has been used to select the next feature for a split; a relevant feature decreases the conditional entropy of the category of the example. Another parameter is maximum depth; it directly relates to overfitting as a large depth means too many conditions need to be satisfied before category of an example if predicted, and too few examples in the leaf nodes. As there are 902 examples in total, the maximum depth of the tree was chosen as 10 - a depth of 8 would result in 256 leaf nodes (for a complete binary tree) with 3.52 examples per leaf node on an average; in reality, the tree is unbalanced with fewer than 256 leaf nodes, so a depth slightly larger than 8 (i.e. 10) has been chosen. Yet another parameter, which also relates to overfitting is the minimum number of examples at a node, required for a split; this has been set to 8 examples. As mentioned before, RF selects the

TABLE 2. Parameters for RF classifier.

Parameter	Value
Criterion to split	Entropy
Max depth	10
Max features	Squared Root
Max leaf nodes	No limit
Min samples to split	8
Number of trees	30

TABLE 3. Parameters used for SVM classifier.

Parameter	Value
C (Regularization parameter)	3
Kernel function	Linear
Maximum iterations	No limit

TABLE 4. Parameters for Naïve Bayes classifier.

Parameter	Value
Prior probability	not considered
Probability density	gaussian

next feature for a split from a subset of features; the number of features in this subset, is set to the square root of total number of features; finally, the number of decision trees to be used in the ensemble, is set to 30.

2) SUPPORT VECTOR MACHINES

Support Vector Machine (SVM) is a discriminative model which seeks out a decision boundary of maximum margin between the classes. In this work, the linear-kernel SVM, which provides a linear decision boundary, has been used. The parameter setting for the SVM has been shown in Table 3.

The decision boundary provided by SVM enables us to predict the category to which an example belongs, from among two classes. However, flooding level detection is a multi-class classification problem. So, a one vs one approach is used; class label is predicted by majority vote over all pairs of classes.

Yet another use of SVM model, in this work, is to find out the most *characterizing* or *relevant* features. SVM computes a decision boundary as shown in Eq. 3:

$$a_0 + a_1 f_1 + a_2 f_2 + \ldots + a_n f_n = 0 \tag{3}$$

where a_i are the coefficients corresponding to feature f_i; the magnitudes $|a_i|$, therefore, indicate the importance of features f_i in the classification task, and larger values of magnitudes may be used to identify relevant or characterizing features.

3) NAÏVE BAYES

Naïve bayes (NB) is a generative model, which classifies with the class having maximum posterior probability for a particular example (from Bayes rule) and assumes independence of features. As features are typically not independent, and may be correlated, principal component analysis (PCA) may be applied in order to obtain an uncorrelated set of features. These features may then be used by the NB model to classify examples. The parameters of the NB model have been shown in Table 4.

TABLE 5. 5-fold cross validation average accuracy for different models.

Model	Class. Accuracy (%)
Random Forest	99.11
SVM	99.45
NB+PCA	95.90

TABLE 6. RF performance.

Category	Precision	Recall	F1 Score
0 feet	1.0000	1.0000	1.0000
0.19 feet	0.9902	0.9907	0.9904
2.5 feet	1.0000	1.0000	1.0000
4.5 feet	0.9954	0.9953	0.9953

TABLE 7. NB + PCA performance.

Category	Precision	Recall	F1 Score
0 feet	0.9462	0.9800	0.9623
0.19 feet	0.9463	0.9206	0.9328
2.5 feet	0.9527	1.0000	0.9749
4.5 feet	0.9754	0.9584	0.9668

TABLE 8. SVM performance.

Category	Precision	Recall	F1 Score
0 feet	1.0000	0.9860	0.9929
0.19 feet	0.9906	0.9955	0.9930
2.5 feet	1.0000	1.0000	1.0000
4.5 feet	0.9927	0.9955	0.9941

C. PERFORMANCE METRICS

The data was split with 80% of the data used for training and the remaining 20% of the data used for testing. The performance metrics used were classification accuracy (percentage of correctly classified examples), precision, recall and F1 score. While classification accuracy was computed by averaging over all classes, precision, recall and F1 score were computed for each class. 5-fold cross validation was used, and performance metrics were averaged over the 5 folds in order to obtain stable estimates.

VIII. PERFORMANCE EVALUATION

In this section, performance of machine learning models is compared followed by a discussion of gait characteristics in different depths and an analysis of relevant features for classification.

A. MODEL PERFORMANCE

The classification accuracy for the models mentioned in Sec. VII-B is shown in the Table 5. The results for individual models are given in Tables 6, 7 and 8. Results indicate that all models perform well on all the classes with SVM, RF models performing better than NB + PCA model. SVM and RF are both discriminative models, while NB is a generative model. The lower performance of NB may be attributed to the assumed Gaussian probability density which may not be true in the case of all features. The models perform well on all the classes. Similar classification accuracies have been reported in the case of other FBAs e.g. HAR [37], detection of a correct repetition in the case of resistance training [38] and identifying ski-skating gears [39].

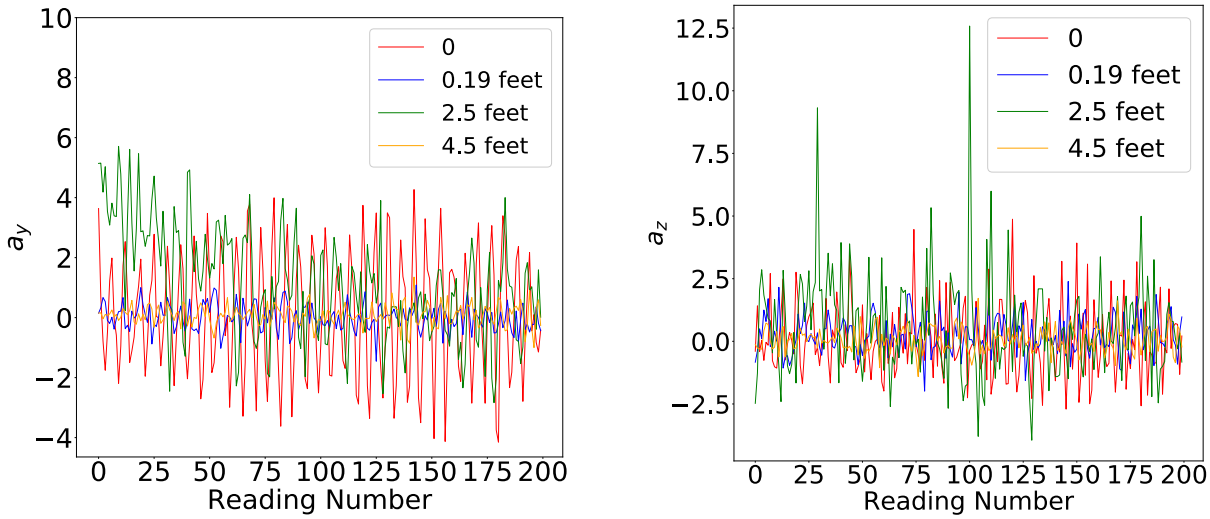

(a) Linear acceleration in the direction of gravity

(b) Linear acceleration in direction of user movement

FIGURE 4. Acceleration patterns in different water depths.

In the succeeding sections, the characteristics of gait in different flooding levels and the relevant features in each case are analyzed.

B. GAIT CHARACTERISTICS IN DIFFERENT DEPTHS

The gait in different depths of water was observed to have different characteristics. Fig. 4 shows the plots of a_y and a_z over a window of 200 points for all depths. It may be noted that a_x, a_y and a_z are directly proportional to the user exertion on the phone (as a consequence of Newton's second law of motion). The different characteristics of a_y and a_z in each of these depths is discussed below:

1) *Land:* The gait on land is characterized by consistent walking pattern when compared to walking in water, and user exertion has a larger magnitude when compared to walking in water as indicated by the plots in Fig. 4. Interleaved exertions in opposite directions (due to both acceleration and deceleration in the same step) results in large variances in accelerations.
2) *0.19ft:* A narrow layer of water on the surface causes the user to exert caution while walking to prevent from slipping, and to prevent water from splashing onto clothes. This results in user exertions of smaller magnitude, and smaller variances in accelerations.
3) *2.5ft:* The user needs to exert a great deal of force to lift his leg up (almost out of the water) and bring it down; lifting the leg up involves overcoming drag force in opposite direction, and bringing the leg down likewise also involves overcoming drag force in opposite direction as shown in Fig. 2c. The same can be said about moving the leg forward (Fig. 2b). This leads to exertions of large magnitudes and variances (Fig. 4).
4) *4.5ft:* Water resistance (i.e drag force and buoyancy) is more in this case, which overwhelms the user, and renders him/her incapable of exerting a large force. This leads to smaller magnitude user exertions interleaved in opposing directions and consequently smaller acceleration variances (Fig. 4).

C. CHARACTERIZING FEATURES

The most characterizing features for each pair of classes may be determined from the one-to-one SVM model, as explained in Sec. VII-B, by using the coefficients of the decision boundary.

Fig. 5 shows a scatterplot for each pair of classes with the two most relevant features on the x and y axes. Fig 5c (0ft vs 4.5ft) indicates that the spectral energy of a_y takes larger values on dry land than on 4.5ft. This means that magnitudes of a_y, and consequently user exertion, are greater for dry land than 4.5ft; this was noted from the discussion in Sec. VIII-B (Fig. 4a); as mentioned before, this is true because user exertion is restricted in 4.5ft deep water. The figure also indicates that a_y, and consequently individual exertion in the direction of gravity, has more variance in dry land than in 4.5ft water; this is true because movement in both upward and downward directions is restricted in 4.5ft water; this difference in variances was also noted in Sec. VIII-B (Fig. 4a). A similar figure is obtained in Fig 5a (land vs 0.19ft); as mentioned in Sec. VIII-B, user exertion is lesser in the case of 0.19ft as individuals are normally more cautious about walking in 0.19ft as a precaution against slipping and to prevent water from splashing onto clothes.

Fig 5b compares gait patterns on land with 2.5ft; it indicates that g_y has a stronger frequency response for land than 2.5ft; this is due to perturbations in water, which result in more erratic walking pattern in 2.5ft water.

Fig. 5d compares 0.19ft with 2.5ft. It indicates that in the case of 0.19ft, g_y has higher values on an average, indicating that the mobile phone is tilted to a smaller extent in 0.19ft than in 2.5ft. Also, g_y has stronger frequency response for 0.19ft than 2.5ft.

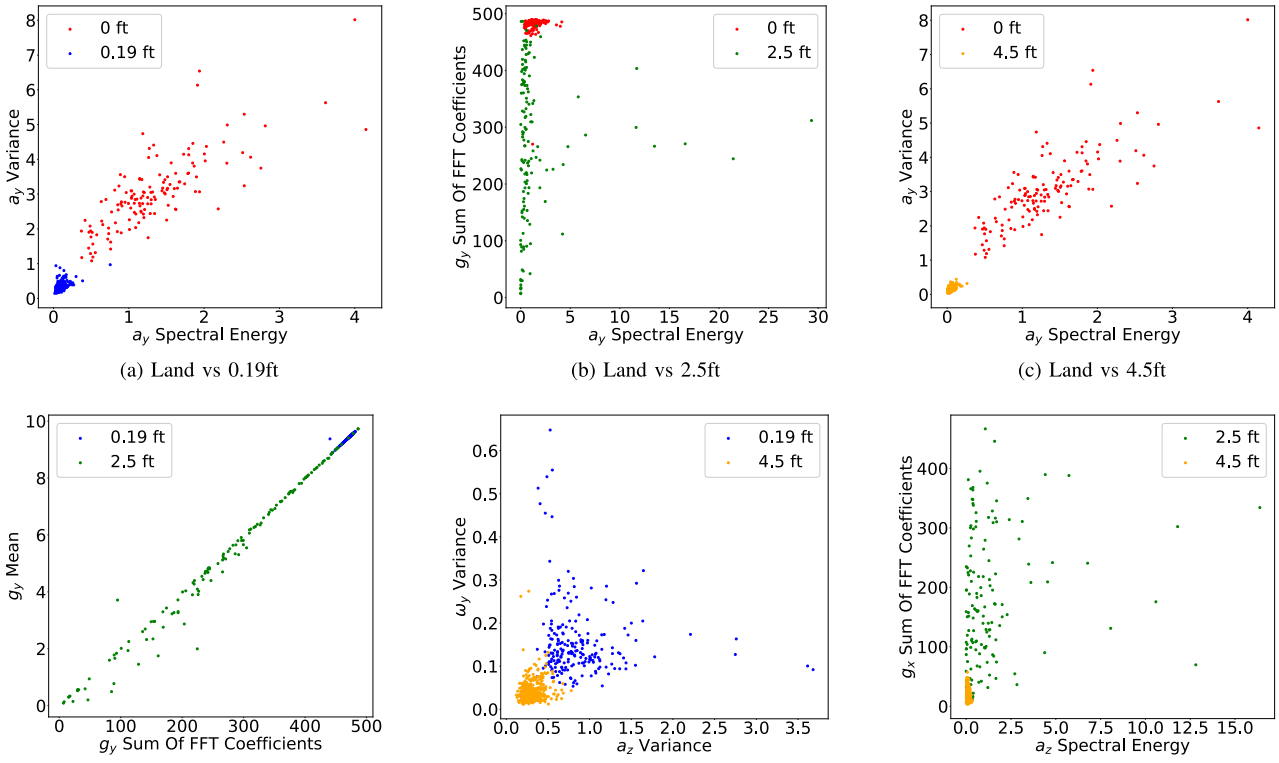

(a) Land vs 0.19ft (b) Land vs 2.5ft (c) Land vs 4.5ft

(d) 0.19ft vs 2.5ft (e) 0.19 vs 4.5 (f) 2.5 vs 4.5

FIGURE 5. **Pairwise scatter plot for each pair of categories using two most relevant features.**

Fig. 5e compares gait patterns for 0.19ft with 4.5ft. It indicates that variance of a_z is usually larger for 0.19ft; this is in in line with the intuition that user exertion in the forward direction has greater variation for 0.19 ft than for 4.5ft; as user exertion in the forward direction is mitigated by high water resistance (i.e drag force) in 4.5ft case. Further, variance of ω_y is usually larger for 0.19ft as compared to 4.5ft; this may also be due to the effect of high water resistance in 4.5ft case.

Fig. 5f compares gait patterns for 2.5ft with 4.5ft. Spectral energy of a_z, which indicates magnitude of user exertion in forward direction, is normally more for 2.5ft as compared to 4.5ft; this is due to the greater water resistance (i.e drag force) in 4.5ft as compared to 2.5ft. Further, frequency response of g_x is usually greater for 2.5ft as compared to 4.5ft; this indicates that the pattern of tilting the smartphone with respect to the earth shows a regular pattern more frequently in the case of 2.5ft.

IX. CONCLUSION

Detecting flooding level in urban areas aids in rushing emergency response to areas of attention. It also aids in improvement of storm water drains in urban areas by identifying congestion points. This work introduces a new technique to detect the flooding level using smartphone sensors; this technique is exempt of additional costs for installation of sensors along the road for flooding-level detection; the ubiquitous nature of smartphones in this generation ensures that data is collected from several locations.

Characteristics of the gait in different water levels were easily distinguished using accelerometer and gyroscope readings, and were using to identify flooding levels. Random forest, SVM and NB classifiers were attempted to predict the flooding level, of which SVM performed best with 99.45% accuracy. The most relevant features for classification match the intuitive understanding of gait in different flooding levels. As future work, other models for classification like kNN, CNN, deep belief networks or HMMs may be attempted.

In this work, prediction of flooding-level, which could be one of four values, has been performed, and this is a classification problem. It may alternatively be treated as a regression problem, and flooding level may be predicted as a continuous value; this would require data from all flooding levels.

To take full advantage of smartphone sensors, the authors believe that a body position independent mechanism should be used; further, flooding level detection should automatically be triggered without user involvement. A combination of the above two features would enable flooding data to be automatically transferred to the central server, leading to the generation of a 'flood map' of the locality. For this approach to be feasible, continuous mobile sensing, and energy efficient mechanisms on the lines of [40] should be used.

Another interesting research direction would be the classification of flooding level using sensor signals picked up from vehicles moving on flooded roads.

ACKNOWLEDGMENT

(Ujjawal K. Panchal and Hardik Ajmani contributed equally to this work.) The authors would like to thank Rajpath Club Ltd., Ahmedabad, and FabHotel Prime The King's Court, Goa, for allowing us to record readings in their pools. They would also like to thank the volunteers H. Panchal, A. Modi, A. Daniel, P. Gandhi, P. Shah, U. Patel, M. Naik, A. Singh, and V. Mehndiratta for volunteering enthusiastically to help with their research.

REFERENCES

[1] D. C. Mason, I. J. Davenport, J. C. Neal, G. J.-P. Schumann, and P. D. Bates, "Near real-time flood detection in urban and rural areas using high-resolution synthetic aperture radar images," *IEEE Trans. Geosci. Remote Sens.*, vol. 50, no. 8, pp. 3041–3052, Aug. 2012.

[2] D. C. Mason, L. Giustarini, J. García-Pintado, and H. L. Cloke, "Detection of flooded urban areas in high resolution synthetic aperture radar images using double scattering," *Int. J. Appl. Earth Observ. Geoinf.*, vol. 28, pp. 150–159, 2014.

[3] M. Shoaib, S. Bosch, O. D. Incel, H. Scholten, and P. J. M. Havinga, "Fusion of smartphone motion sensors for physical activity recognition," *Sensors*, vol. 14, no. 6, pp. 10146–10176, 2014.

[4] Press Information Bureau. (Oct. 27, 2016). *Interview: Dr. Kapil Gupta on Urban Floods*. Accessed: Oct. 1, 2019. [Online]. Available: https://pib.gov.in/newsite/printrelease.aspx?relid=153050

[5] C. S. Kotteswaran. (Dec. 6, 2016). *Tamil Nadu: Chennai Floods Cause a Loss of Rs 50,000-cr*. Deccan Chronicle. Accessed: Oct. 1, 2019. [Online]. Available: https://www.deccanchronicle.com/151206/nation-current-affairs/article/chennai-floods-caused-loss-50-thousand-crore

[6] D. M. Karantonis, M. R. Narayanan, M. Mathie, N. H. Lovell, and B. G. Celler, "Implementation of a real-time human movement classifier using a triaxial accelerometer for ambulatory monitoring," *IEEE Trans. Inf. Technol. Biomed.*, vol. 10, no. 1, pp. 156–167, Jan. 2006.

[7] A. Samà, C. Pérez-Lopez, J. Romagosa, D. Rodríguez-Martín, A. Català, J. Cabestany, D. A. Pérez-Martínez, and A. Rodríguez-Molinero, "Dyskinesia and motor state detection in Parkinson's disease patients with a single movement sensor," in *Proc. Annu. Int. Conf. IEEE Eng. Med. Biol. Soc.*, Aug./Sep. 2012, pp. 1194–1197.

[8] F. Bianchi, S. J. Redmond, M. R. Narayanan, S. Cerutti, B. G. Celler, and N. H. Lovell, "Falls event detection using triaxial accelerometry and barometric pressure measurement," in *Proc. Annu. Int. Conf. IEEE Eng. Med. Biol. Soc.*, Sep. 2009, pp. 6111–6114.

[9] Y.-L. Hsu, S.-C. Yang, H.-C. Chang, and H.-C. Lai, "Human daily and sport activity recognition using a wearable inertial sensor network," *IEEE Access*, vol. 6, pp. 31715–31728, 2018.

[10] M. B. D. Rosario, S. J. Redmond, and N. H. Lovell, "Tracking the evolution of smartphone sensing for monitoring human movement," *IEEE Sensors*, vol. 15, no. 8, pp. 18901–18933, Jul. 2015.

[11] S. A. Antos, M. V. Albert, and K. P. Kording, "Hand, belt, pocket or bag: Practical activity tracking with mobile phones," *J. Neurosci. Methods*, vol. 231, pp. 22–30, Jul. 2014.

[12] Y. He and Y. Li, "Physical activity recognition utilizing the built-in kinematic sensors of a smartphone," *Int. J. Distrib. Sensor Netw.*, vol. 9, no. 4, 2013, Art. no. 481580.

[13] E. Mitchell, D. Monaghan, and N. O'Connor, "Classification of sporting activities using smartphone accelerometers," *Sensors*, vol. 13, no. 4, pp. 5317–5337, 2013.

[14] M. Kranz, A. Möller, N. Hammerla, S. Diewald, T. Plötz, P. Olivier, and L. Roalter, "The mobile fitness coach: Towards individualized skill assessment using personalized mobile devices," *Pervasive Mobile Comput.*, vol. 9, no. 2, pp. 203–215, 2013.

[15] W. Tao, T. Liu, R. Zheng, and H. Feng, "Gait analysis using wearable sensors," *Sensors*, vol. 12, no. 12, pp. 2255–2283, 2012.

[16] J. Juen, Q. Cheng, V. Prieto-Centurion, J. A. Krishnan, and B. Schatz, "Health monitors for chronic disease by gait analysis with mobile phones," *Telemedicine e-Health*, vol. 20, no. 11, pp. 1035–1041, 2014.

[17] A. J. A. Majumder, F. Rahman, I. Zerin, W. Ebel, Jr., and S. I. Ahamed, "iPrevention: Towards a novel real-time smartphone-based fall prevention system," in *Proc. 28th Annu. ACM Symp. Appl. Comput.*, 2013, pp. 513–518.

[18] P. Raknim and K.-C. Lan, "Gait monitoring for early neurological disorder detection using sensors in a smartphone: Validation and a case study of parkinsonism," *Telemed. e-Health*, vol. 22, no. 1, pp. 75–81, Jan. 2016.

[19] T. T. Ngo, Y. Makihara, H. Nagahara, Y. Mukaigawa, and Y. Yagi, "The largest inertial sensor-based gait database and performance evaluation of gait-based personal authentication," *Pattern Recognit.*, vol. 47, no. 1, pp. 228–237, 2014.

[20] R. Damaševicius, R. Maskeliunas, A. Venckauskas, and M. Wozniak, "Smartphone user identity verification using gait characteristics," *Symmetry*, vol. 8, no. 10, p. 100, 2016.

[21] Z. Arnold, D. Larose, and E. Agu, "Smartphone inference of alcohol consumption levels from gait," in *Proc. Int. Conf. Healthcare Inform.*, 2015, pp. 417–426.

[22] Y. Ren, Y. Chen, M. C. Chuah, and J. Yang, "Smartphone based user verification leveraging gait recognition for mobile healthcare systems," in *Proc. IEEE Int. Conf. Sens., Commun. Netw. (SECON)*, Jun. 2013, pp. 149–157.

[23] M. Gadaleta and M. Rossi, "IDNet: Smartphone-based gait recognition with convolutional neural networks," *Pattern Recognit.*, vol. 74, pp. 25–37, Feb. 2018.

[24] N. Neverova, C. Wolf, G. Lacey, L. Fridman, D. Chandra, B. Barbello, and G. Taylor, "Learning human identity from motion patterns," *IEEE Access*, vol. 4, pp. 1810–1820, 2016.

[25] B. Sun, Y. Wang, and J. Banda, "Gait characteristic analysis and identification based on the iPhone's accelerometer and gyrometer," *Sensors*, vol. 14, no. 9, pp. 17037–17054, 2014.

[26] A. Anjum and M. U. Ilyas, "Activity recognition using smartphone sensors," in *Proc. IEEE 10th Consum. Commun. Netw. Conf. (CCNC)*, Jan. 2013, pp. 914–919.

[27] M. Shoaib, H. Scholten, and P. J. M. Havinga, "Towards physical activity recognition using smartphone sensors," in *Proc. IEEE 10th Int. Conf. Ubiquitous Intell. Comput., IEEE 10th Int. Conf. Auton. Trusted Comput.*, Dec. 2013, pp. 80–87.

[28] W. Wu, S. Dasgupta, E. E. Ramirez, C. Peterson, and G. J. Norman, "Classification accuracies of physical activities using smartphone motion sensors," *J. Med. Internet Res.*, vol. 14, no. 5, p. e130, 2012.

[29] A. Wang, G. Chen, J. Yang, S. Zhao, and C.-Y. Chang, "A comparative study on human activity recognition using inertial sensors in a smartphone," *IEEE Sensors J.*, vol. 16, no. 11, pp. 4566–4578, Jun. 2016.

[30] M. M. Hassan, M. Z. Uddin, A. Mohamed, and A. Almogren, "A robust human activity recognition system using smartphone sensors and deep learning," *Future Gener. Comput. Syst.*, vol. 81, pp. 307–313, Apr. 2018.

[31] J.-L. Reyes-Ortiz, L. Oneto, A. Samà, X. Parra, and D. Anguita, "Transition-aware human activity recognition using smartphones," *Neurocomputing*, vol. 171, pp. 754–767, Jan. 2016.

[32] S. Dernbach, B. Das, N. C. Krishnan, B. L. Thomas, and D. J. Cook, "Simple and complex activity recognition through smart phones," in *Proc. 8th Int. Conf. Intell. Environ.*, 2012, pp. 214–221.

[33] Y. Chen and C. Shen, "Performance analysis of smartphone-sensor behavior for human activity recognition," *IEEE Access*, vol. 5, pp. 3095–3110, 2017.

[34] C. A. Ronao and S.-B. Cho, "Human activity recognition with smartphone sensors using deep learning neural networks," *Expert Syst. Appl.*, vol. 59, pp. 235–244, Oct. 2016.

[35] Y.-S. Lee and S.-B. Cho, "Activity recognition using hierarchical hidden Markov models on a smartphone with 3D accelerometer," in *Proc. Int. Conf. Hybrid Artif. Intell. Syst.* Berlin, Germany: Springer, 2011, pp. 460–467.

[36] A. M. Khan, M. H. Siddiqi, and S.-W. Lee, "Exploratory data analysis of acceleration signals to select light-weight and accurate features for real-time activity recognition on smartphones," *Sensors*, vol. 13, no. 10, pp. 13099–13122, 2013.

[37] B. Aguiar, J. Silva, T. Rocha, S. Carneiro, and I. Sousa, "Monitoring physical activity and energy expenditure with smartphones," in *Proc. IEEE-EMBS Int. Conf. Biomed. Health Inform. (BHI)*, Jun. 2014, pp. 664–667.

[38] I. Pernek, K. A. Hummel, and P. Kokol, "Exercise repetition detection for resistance training based on smartphones," *Pers. Ubiquitous Comput.*, vol. 17, no. 4, pp. 771–782, 2013.

[39] T. Stöggl, A. Holst, A. Jonasson, E. Andersson, T. Wunsch, C. Norström, and H.-C. Holmberg, "Automatic classification of the sub-techniques (gears) used in cross-country ski skating employing a mobile phone," *Sensors*, vol. 14, no. 11, pp. 20589–20601, 2014.

[40] Z. Yan, V. Subbaraju, D. Chakraborty, A. Misra, and K. Aberer, "Energy-efficient continuous activity recognition on mobile phones: An activity-adaptive approach," in *Proc. 16th Int. Symp. Wearable Comput.*, 2012, pp. 17–24.

UJJAWAL K. PANCHAL (M'19) was born in Ahmedabad, India, in August 1998. He is currently pursuing the Bachelors of Technology degree incomputer science engineering with the SRM Institute of Science and Technology, Chennai, India.

He was a winter intern with the National University of Singapore and Hewlett Packard Enterprise, Singapore from December 2017 to January 2018. From May 2018 to July 2018 and December 2018 to Janurary 2019, he worked as a Research Intern with the Indian Institute of Management, Ahmedbabad. During his time at IIMA, he wrote a research article titled Identification of Potential Future Credit Card Defaulters from Non Defaulters using Self Organizing Maps which he presented at the 10th International Conference on Computing, Communication and Networking Technologies 2019. He is currently interests include machine learning, deep learning, and data science research.

HARDIK AJMANI was born in Haryana, India, in April 1998. He is currently pursuing the Bachelor of Technology degree in computer science and engineering with SRM Institute of Science and Technology, Chennai, India, which he joined, in 2016.

He worked as a Software Services Intern with eClerx Private Ltd., Navi Mumbai, India, in June 2017. He worked as a summer trainee in Trio Motions Private Ltd., Pune, India, in June 2018, and Asia University, Taiwan, in July 2018. His current research interests include deep learning.

SAAD Y. SAIT (M'16) was born in Chennai, India, in 1976. He received the B.E. degree in computer science from the Birla Institute of Technology and Science, India, in 1998, the M.S.E. degree in computer and information science from the University of Pennsylvania, Philadelphia, USA, in 1999, and the Ph.D. degree in computer science and engineering from the Indian Institute of Technology, Madras, India, in 2017.

From 2000 to 2002, he was an Associate Software Engineer with Syncsort Incorporated, USA. From 2003 to 2010, he was a Lecturer with the MEASI Institute of Information Technology. Since 2017, he has been a Research Associate Professor with the SRM Institute of Science and Technology, Chennai, India. His current research interests include text classification and filtering, activity recognition using smartphone sensors, and machine learning.